NOAA TR NOS 43

A UNITED STATES
DEPARTMENT OF
COMMERCE
PUBLICATION

NOAA Technical Report NOS 43

U.S. DEPARTMENT OF COMMERCE
National Oceanic and Atmospheric Administration
National Ocean Survey

Phase Correction for Sun-Reflecting Spherical Satellite

ERWIN SCHMID

ROCKVILLE, MD.
August 1971

NOAA TECHNICAL REPORTS

National Ocean Survey Series

The National Ocean Survey (NOS) provides charts and related information for the safe navigation of marine and air commerce. The Survey also furnishes other earth science data — from geodetic, hydrographic, oceanographic, geomagnetic, seismologic, gravimetric, and astronomic surveys, observations, investigations, and measurements — to protect life and property and to meet the needs of engineering, scientific, defense, commercial, and industrial interests.

Because many of these reports deal with new practices and techniques, the views expressed are those of the authors, and do not necessarily represent final Survey policy. NOS series of NOAA Technical Reports is a continuation of, and retains the consecutive numbering sequence of, the former series, ESSA Technical Report Coast and Geodetic Survey (C&GS), and the earlier series, C&GS Technical Bulletin.

Reports in the series are available through the Superintendent of Documents, U.S. Government Printing Office, Washington, D.C. 20402. Those publications marked by an asterisk are out of print.

COAST AND GEODETIC SURVEY TECHNICAL BULLETINS

*C&GS 1. Aerotriangulation Adjustment of Instrument Data by Computational Methods. William D. Harris, January 1958. (Superseded by No. 23.)

*C&GS 2. Tellurometer Traverse Surveys. Lt. Hal P. Demuth, March 1958.

*C&GS 3. Recent Increases in Coastal Water Temperature and Sea Level—California to Alaska. H. B. Stewart, Jr., B. D. Zetler, and C. B. Taylor, May 1958.

*C&GS 4. Radio Telemetry Applied to Survey Problems. Richard R. Ross, February 1959.

*C&GS 5. Raydist on Georges Bank. Capt. Gilbert R. Fish, April 1959.

*C&GS 6. The Tsunami of March 9, 1957, as Recorded at Tide Stations. Garrett G. Salsman, July 1959.

*C&GS 7. Pantograph Adjustment. G. C. Tewinkel, July 1959.

*C&GS 8. Mathematical Basis of Analytic Aerotriangulation. G. C. Tewinkel, August 1959. (Superseded by No. 21.)

*C&GS 9. Gravity Measurement Operations in the Field. Lt. Comdr. Hal P. Demuth, September 1959.

*C&GS 10. Vertical Adjustment of Instrument Aerotriangulation by Computational Methods. William B. Harris, September 1959. (Superseded by No. 23.)

*C&GS 11. Use of Near-Earth Satellite Orbits for Geodetic Information. Paul D. Thomas, January 1960.

*C&GS 12. Use of Artificial Satellites for Navigation and Oceanographic Surveys. Paul D. Thomas, July 1960.

C&GS 13. A Singular Geodetic Survey. Lansing G. Simmons, September 1960. Price $0.15.

*C&GS 14. Film Distortion Compensation for Photogrammetric Use. G. C. Tewinkel, September 1960.

*C&GS 15. Transformation of Rectangular Space Coordinates. Erwin Schmid, December 1960.

*C&GS 16. Erosion and Sedimentation—Eastern Chesapeake Bay at the Choptank River. G. F. Jordan, January 1961.

*C&GS 17. On the Time Interval Between Two Consecutive Earthquakes. Tokuji Utsu, February 1961.

*C&GS 18. Submarine Physiography of the U.S. Continental Margins. G. F. Jordan, March 1962.

*C&GS 19. Analytic Absolute Orientation in Photogrammetry. G. C. Tewinkel, March 1962.

*C&GS 20. The Earth as Viewed from a Satellite. Erwin Schmid, April 1962.

*C&GS 21. Analytic Aerotriangulation. W. D. Harris, G. C. Tewinkel, and C. A. Whitten, July 1962. (Corrected July 1963.)

*C&GS 22. Tidal Current Surveys by Photogrammetric Methods. Morton Keller, October 1963.

*C&GS 23. Aerotriangulation Strip Adjustment. M. Keller and G. C. Tewinkel, August 1964.

*C&GS 24. Satellite Triangulation in the Coast and Geodetic Survey. February 1965.

*C&GS 25. Aerotriangulation: Image Coordinate Refinement. M. Keller and G. C. Tewinkel, March 1965.

*C&GS 26. Instrumented Telemetering Deep Sea Buoys. H. W. Straub, J. M. Arthaber, A. L. Copeland, and D. T. Theodore, June 1965.

*C&GS 27. Survey of the Boundary Between Arizona and California. Lansing G. Simmons, August 1965.

*C&GS 28. Marine Geology of the Northeastern Gulf of Maine. R. J. Malloy and R. N. Harbison, February 1966.

C&GS 29. Three-Photo Aerotriangulation. M. Keller and G. C. Tewinkel, February 1966. Price $0.35.

(Continued on inside back cover)

U.S. DEPARTMENT OF COMMERCE
Maurice H. Stans, Secretary
NATIONAL OCEANIC AND ATMOSPHERIC ADMINISTRATION
Robert M. White, Administrator
NATIONAL OCEAN SURVEY
Don A. Jones, Director

NOAA Technical Report NOS 43

Phase Correction for Sun-Reflecting Spherical Satellite

ERWIN SCHMID

GEODETIC RESEARCH AND DEVELOPMENT LABORATORY

ROCKVILLE, MD.
AUGUST 1971

UDC 528.225:521.61

528	Geodesy
.2	Earth measurement
.22	Methods of determining the figure of the earth
.225	Astronomical methods; irregularities of lunation
521.61	Orbital motions of satellite

For sale by the Superintendent of Documents, U.S. Government Printing Office
Washington, D.C. 20402—Price .25 cents. Stock Number 0321-0004.

Contents

LIST OF FIGURES

Phase Correction for Sun-Reflecting Spherical Satellite

Erwin Schmid
Geodetic Research and Development Laboratory
National Oceanic Survey

ABSTRACT. Correction formulas are developed that convert the ground-based camera measurements of the direction to the center of the light source on a balloon-type, spherical satellite to the corresponding direction to the geometrical center of the satellite. The correction is necessary because, in the case of a diffusively reflecting satellite, the photographed satellite image refers to the visible sun-illuminated portion of the satellite surface and, for specular reflection, to the location of the sun's image on the balloon. The correction is small but, as a computable bias, is incorporated in the mathematical model of the Geometric Satellite Triangulation World Net Program.

INTRODUCTION

In the Geometric Satellite Triangulation World Net Program (for which field operations were concluded late in 1970) and in the North American Densification Net Program (now in progress), sunlight-reflective balloon satellites, 100 ft in diameter, such as the NASA-launched Echo I, Echo II, and, at present, PAGEOS (Passive Geodetic Satellite), are photographed simultaneously from two or more ground sites against the background of surrounding stars for the purpose of locating these camera stations in the three-dimensional static flat space defined in part by the right ascension-declination system of metric astronomy. An exposition of the method in detail is being prepared for publication by the Office of the National Geodetic Survey, a component of NOAA's National Ocean Survey.

The light energy of the sun reflected from the moving satellite creates a track on the camera plate which is chopped by camera shutters into a series of point-like images, each of which represents a position of the satellite in space at an instant determined by the associated electronic timing system. The measured plate coordinates of the centroid of such an image are transformed into space coordinates of the light source (at the satellite) for the specific image. It is the purpose of this report to find the center of this light source on the satellite and hence to compute a correction that displaces it to the geometrical center of the balloon as a common target for all stations. If, as in the case of Echo II, the portion of the balloon surface illuminated by the sun and facing the camera site reflects the sunlight diffusely, the light energy sensitizing the plate comes more or less uniformly from all parts of what would appear to the eye, if sufficiently magnified, as a crescent analogous to the moon's appearance. The specular reflective surfaces of Echo I and PAGEOS concentrate the source of light energy in a point on the balloon surface. Pertinent corrections are developed separately.

These corrections are small, but they represent a computable bias and are incorporated in the mathematical model of the Geometric Satellite Triangulation World Net Program.

DIFFUSIVE REFLECTION

The portion of a satellite's sun-illuminated hemisphere facing an observer changes continuously with time in the same manner and for the same reason that the moon goes through its phases. Figure 1 shows the spherical satellite with radius ρ and center P. If the direction to the sun points to S on the sphere, then the illuminated half is bounded by the great circle DBC whose pole is S. The direction to the observer is E, and, at great distances, his outline of the satellite is the great circle CAD for which E is the pole. This aspect from the earth is shown in figure 2, which is figure 1 viewed from below. The visible illuminated portion of the satellite consists of the spherical triangle

Figure 1.—Phase angle of spherical satellite.

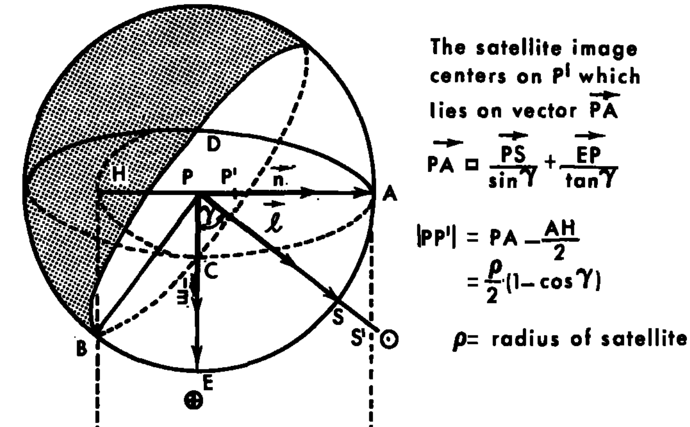

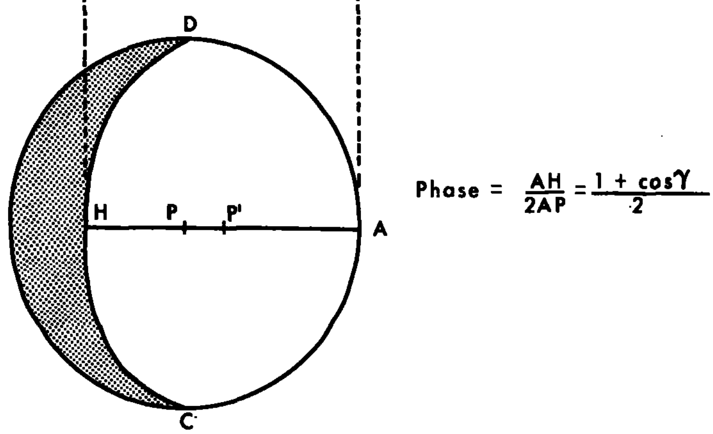

Figure 2.—Appearance from earth of "moon" phase.

DAB in figure 1 and its symmetrical counterpart triangle CAB.

The angle γ at the satellite, between the direction to the sun and to the observer, is defined as the phase angle. Its range is from 0° to 180°, producing at these limits full moon and new moon, respectively. The phase itself is defined with respect to the projection of the illuminated portion onto the plane ACD as depicted in figure 2; it is directly proportional to the amount of illumination reaching the earth (its relative magnitude) and is equal to the ratio AH/2AP of these two segments in figures 1 and 2.

From figure 1, we have

$$PH = PB \cos \angle BPH = \rho \cos \gamma.$$

Hence, from figure 2,

$$\text{Phase} = \frac{AH}{2AP} = \frac{AP + PH}{2AP}$$

$$= \frac{\rho + \rho \cos \gamma}{2\rho} = \frac{1 + \cos \gamma}{2}.$$

Assuming the sun's light to be diffused in all directions from the satellite's surface, the source of the light energy creating the satellite image may be postulated to originate from a point P' at the midpoint of segment AH. Because the phase is generally different for the several camera stations, in addition to being variable with time, it is necessary to transform the point P' to a point on the satellite invariant with respect to phase, such as its center P, to achieve coincidence in space and time for each of the images photographed from different locations. The purpose here is to evaluate the effect of the shift of the observation from its source P' to the geometrical center P of the satellite, in other words, the effect of the displacement vector $P'P$ on the position vector camera-satellite. It should be noted that this increment is sufficiently small to be treated as a first-order differential; except for sign, it is immaterial whether this correction is added to the direction to P' or to the direction to P.

The direction cosines of a line in space relative to a specified Cartesian coordinate system (XYZ or $X_1X_2X_3$) are the cosines of the three angles which the line makes with the three axes in the specified order. The direction cosines are also the three projections (inner or dot product) onto these axes of a unit vector associated with this line, that is, the Cartesian components of the vector. Figure 3 shows still a third approach which is convenient for converting astronom-

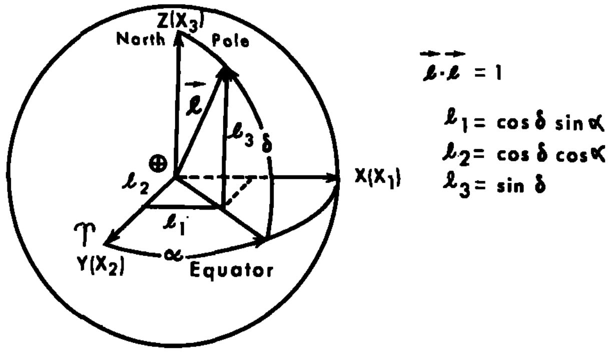

Figure 3.—Direction cosines as Cartesian coordinates on unit sphere.

ical (spherical) coordinates to vector components or Cartesian coordinates. If a sphere of radius one is assumed to be drawn around the origin of the Cartesian coordinate system, then any radius vector of the sphere will be a unit vector, and conversely. Thus, the *XYZ* coordinates of the end point of a radius vector, such as **l**, will be the direction cosines l_1, l_2, l_3 of the corresponding line in space as well as the components of the vector.

One small difference in these different approaches may be noted: In ordinary analytical geometry, the ambiguity arising from the three direction angles and their supplements is left unresolved so that a set of three direction cosines is interchangeable with the set having the opposite sign. This is not permissible in the vectorial approach.

The Cartesian coordinate system of figure 3 is a left-hand, geocentric, inertial system; that is, the origin is at the center of the earth, the *Z*-axis points north, and the *Y*-axis is directed toward the vernal equinox. In this system, the apparent right ascension and declination of an object in space are, except for parallax, the angles α and δ indicated in the figure.

For an object as distant as the sun, α and δ as seen from the satellite are sufficiently close for the purpose (maximum parallax$\sim$10 seconds of arc) to use the geocentric coordinates $\alpha_\odot$, $\delta_\odot$ directly from the ephemeris. Using these values, it follows from figure 3 that the direction cosines of the line earth-sun and, specifically, the components of the unit vector in the direction from earth to sun in the geocentric system or in any near-earth, space-parallel system, are

$$\begin{cases} l_1 = \cos\delta_\odot \sin\alpha_\odot \\ l_2 = \cos\delta_\odot \cos\alpha_\odot \\ l_3 = \sin\delta_\odot. \end{cases} \tag{1}$$

The direction from the camera station to the satellite is normally computed in terms of azimuth and elevation with respect to a local horizonal system. The geodetic coordinates of the station are used to convert the azimuth and elevation into corresponding right ascension and declination. The latter are coordinates in the spherical reference system that corresponds directly to the geocentric Cartesian system.

Thus, if this apparent right ascension and declination are α and δ, respectively, then the unit vector **m** in the direction from the camera to the satellite (direction *EP* in fig. 1) has components

$$\begin{cases} m_1 = \cos\delta \sin\alpha \\ m_2 = \cos\delta \cos\alpha \\ m_3 = \sin\delta; \end{cases} \tag{2}$$

and the unit vector in the opposite direction, that is, from *P* to *E*, has the same numerical components with the opposite sign. In other words, the unit vector in the direction of the satellite-camera is $-\mathbf{m}$.

The cosine of the phase angle γ is therefore $-\mathbf{m}\cdot\mathbf{l}$ or

$$\cos\gamma = -(l_1m_1 + l_2m_2 + l_3m_3). \tag{3}$$

Let the unit vector in the direction *PP′* of figure 1 be designated **n**. Because **n** lies in the plane of the unit vector to the sun **l** and the unit vector to the observer $-\mathbf{m}$, it is a linear combination of these, or

$$\mathbf{n} = \lambda\mathbf{l} + \mu\mathbf{m}$$

where λ, μ are undetermined scalars.

The scalar product of this last equation with **m** and **l** gives

$$\mathbf{m}\cdot\mathbf{n} = 0 = \lambda\mathbf{l}\cdot\mathbf{m} + \mu\mathbf{m}\cdot\mathbf{m} = -\lambda\cos\gamma + \mu$$

$$\mathbf{l}\cdot\mathbf{n} = \cos\left(\frac{\pi}{2} - \gamma\right) = \sin\gamma$$
$$= \lambda\mathbf{l}\cdot\mathbf{l} + \mu\mathbf{m}\cdot\mathbf{l} = \lambda - \mu\cos\gamma.$$

From these two equations,

$$\begin{cases} 0 = -\lambda\cos\gamma + \mu \\ \sin\gamma = \lambda - \mu\cos\gamma, \end{cases}$$

we find $\lambda = \csc\gamma$, $\mu = \cot\gamma$ so that

$$\mathbf{n} = (\csc\gamma)\mathbf{l} + (\cot\gamma)\mathbf{m}. \tag{4}$$

This result is also readily apparent from figure 1 as

$$PA = PS + S'A$$

where S' is the intersection of the line *PS* extended with the tangent to the circle at *A*. Scaling the figure down from radius ρ to radius unity, the directed distances *PA*, *PS*, *PE* become the unit vectors **n**, **l**, $-\mathbf{m}$, respectively. From triangle *PAS′*, the length of *PS′*

is csc γ and the length of $S'A$ is cot γ. Therefore, we have

$$PS' = \csc\gamma\mathbf{l}$$

and
$$S'A = \cot\gamma\mathbf{m}$$

because the direction of $S'A$ is opposite to PE. The above vector equation is therefore the equation (4).

The components of $\mathbf{n}$ from equation (4) are

$$\begin{cases} n_1 = \dfrac{l_1 + m_1 \cos\gamma}{\sin\gamma} \\ n_2 = \dfrac{l_2 + m_2 \cos\gamma}{\sin\gamma} \\ n_3 = \dfrac{l_3 + m_3 \cos\gamma}{\sin\gamma} \end{cases} \tag{5}$$

The length of the segment PP' is, from figure 1 or 2,

$$\begin{aligned} |PP'| &= AP - \frac{1}{2}AH \\ &= \rho - \frac{1}{2}(\rho + \rho\cos\gamma) \\ &= \frac{\rho}{2}(1 - \cos\gamma), \end{aligned} \tag{6}$$

so that the vector $PP' = \frac{\rho}{2}(1 - \cos\gamma)\mathbf{n}$

and
$$\text{vector } P'P = \frac{\rho}{2}(\cos\gamma - 1)\mathbf{n}. \tag{7}$$

The unit vector $\mathbf{m}$ in the direction of the satellite is given with equations (2) as a function of right ascension and declination. We consider now the effect on this α and δ of a differential displacement $d\mathbf{m}$ of the vector. From equations (2), it follows that

$$\begin{cases} dm_1 = \cos\alpha\cos\delta\, d\alpha - \sin\alpha\sin\delta\, d\delta \\ dm_2 = -\sin\alpha\cos\delta\, d\alpha - \cos\alpha\sin\delta\, d\delta \\ dm_3 = \cos\delta\, d\delta. \end{cases} \tag{8}$$

Because the components of a unit vector are functionally related, only two of these equations are needed to solve for $d\alpha$ and $d\delta$. We choose the first two for this purpose to obtain a more symmetrical result and get

$$\begin{cases} d\alpha = \dfrac{\cos\alpha}{\cos\delta}dm_1 - \dfrac{\sin\alpha}{\cos\delta}dm_2 \\ d\delta = -\dfrac{\sin\alpha}{\sin\delta}dm_1 - \dfrac{\cos\alpha}{\sin\delta}dm_2. \end{cases} \tag{9}$$

From the relation $m_1^2 + m_2^2 + m_3^2 = 1$, it follows that $\quad m_1dm_1 + m_2dm_2 + m_3dm_3 = 0.$

The left side of this equation can be interpreted as the inner product of the vectors $\mathbf{m}$ and $d\mathbf{m}$. Hence, the differential increment of a unit vector or, for that matter, of any vector of constant length is in a plane normal to the vector.

The phase correction vector $P'P$ satisfies this condition and is sufficiently small to be treated as a differential. If the distance to the satellite is the scalar D, then the position vector is $D\mathbf{m}$ and its differential is $Dd\mathbf{m}$. Setting this differential equal to the vector $P'P$ from equation (7), we obtain

$$d\mathbf{m} = \frac{\rho}{2D}(\cos\gamma - 1)\mathbf{n}.$$

From equations (5), the components of this vector are

$$\begin{cases} dm_1 = \dfrac{\rho(\cos\gamma - 1)}{2D\sin\gamma}(l_1 + m_1\cos\gamma) \\ dm_2 = \dfrac{\rho(\cos\gamma - 1)}{2D\sin\gamma}(l_2 + m_2\cos\gamma) \\ dm_3 = \dfrac{\rho(\cos\gamma - 1)}{2D\sin\gamma}(l_3 + m_3\cos\gamma), \end{cases} \tag{10}$$

which, when substituted in equations (9), give

$$d\alpha = \frac{\rho(\cos\gamma - 1)}{2D\sin\gamma\cos\delta}[\cos\alpha(l_1 + m_1\cos\gamma) - \sin\alpha(l_2 + m_2\cos\gamma)]$$

$$d\delta = \frac{\rho(\cos\gamma - 1)}{2D\sin\gamma\sin\delta}[\sin\alpha(l_1 + m_1\cos\gamma) + \cos\alpha(l_2 + m_2\cos\gamma)].$$

Using equations (1) and (2), the quantity in brackets in $d\alpha$ becomes

$$\begin{aligned} &l_1\cos\alpha - l_2\sin\alpha + \cos\gamma(m_1\cos\alpha - m_2\sin\alpha) \\ &= \cos\delta_\odot\sin\alpha_\odot\cos\alpha - \cos\delta_\odot\sin\alpha + \cos\gamma\cdot 0 \\ &= \cos\delta_\odot\sin(\alpha_\odot - \alpha), \end{aligned}$$

and in $d\delta$ becomes

$$\begin{aligned} &l_1\sin\alpha + l_2\cos\alpha + \cos\gamma(m_1\sin\alpha + m_2\cos\alpha) \\ &= \cos\delta_\odot\sin\alpha_\odot\sin\alpha + \cos\delta_\odot\cos\alpha_\odot\cos\alpha \\ &\quad + \cos\gamma\cos\delta \\ &= \cos\delta_\odot\cos(\alpha_\odot - \alpha) + \cos\gamma\cos\delta. \end{aligned}$$

The corrections to be added to the observed α and δ of a satellite are therefore

$$\begin{cases} d\alpha = \dfrac{\rho(\cos\gamma - 1)}{2D\sin\gamma\cos\delta}\cos\delta_\odot\sin(\alpha_\odot - \alpha) \\ d\delta = \dfrac{\rho(\cos\gamma - 1)}{2D\sin\gamma\sin\delta}(\cos\delta_\odot\cos(\alpha_\odot - \alpha) + \cos\gamma\cos\delta), \end{cases} \tag{11}$$

with ρ = radius of satellite,
D = distance of satellite from the camera,
$\cos\gamma$ is obtained from equation (3), and
$\alpha_\odot$, $\delta_\odot$ are right ascension and declination of the

sun interpolated from the sun's ephemeris for the time of observation.

Because the corrections in equations (11) are small, a single entry in the ephemeris for the middle of the observation period will be sufficient, with $\alpha_\odot$ and $\delta_\odot$ extracted to the nearest 5 seconds of time.

SPECULAR REFLECTION

Equations (11) apply to the case of a spherical satellite which, because of surface irregularities, diffuses light in all directions and hence from all portions of the illuminated surface.

According to Snell's law, a parallel beam of light is reflected in a prescribed direction from a sphere at only one point of the surface. This point lies in the plane of the incident beam and of the radius parallel to the given direction so that its surface normal, a radius, also lies in this plane and bisects the angle between the incident and reflected ray.

In figure 4, which is similar to figure 1, PF is the radius of the sphere which bisects the angle γ and hence is also the angle at F formed by the incident ray from the sun and by the given direction of the observer. A distant, perfectly reflective, spherical satellite appears therefore as a point source of light, transversely displaced from its center by a distance $P''P =$

$$P''P = \rho \sin \gamma/2 = \rho\left(\frac{1-\cos\gamma}{2}\right)^{1/2}.$$

The corrections to α and δ are consequently the corrections in equations (11) of the diffusive case multiplied by the ratio

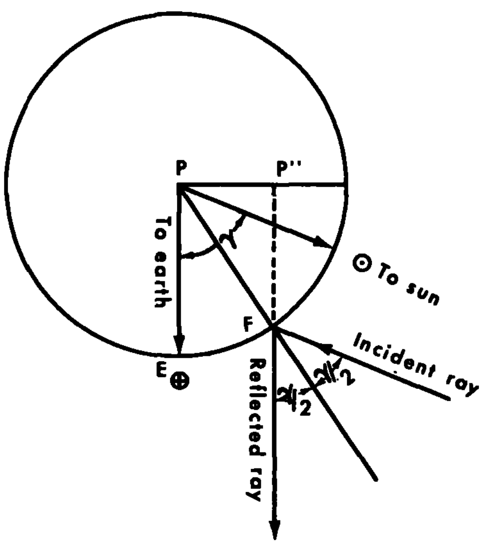

Figure 4.—Specular reflection from a spherical satellite.

$$\frac{PP''}{PP'} = \left(\frac{1-\cos\gamma}{2}\right)^{1/2}\left(\frac{1-\cos\gamma}{2}\right)^{-1} = \left(\frac{1-\cos\gamma}{2}\right)^{1/2},$$

or directly

$$\left\{\begin{aligned} d\alpha &= -\frac{\rho}{D\sin\gamma\cos\delta}\left(\frac{1-\cos\gamma}{2}\right)^{1/2} \cos\delta_\odot \sin(\alpha_\odot-\alpha) \\ d\delta &= \frac{\rho}{D\sin\gamma\sin\delta}\left(\frac{1-\cos\gamma}{2}\right)^{1/2} (\cos\delta_\odot\cos(\alpha_\odot-\alpha) + \cos\gamma\cos\delta). \end{aligned}\right. \tag{12}$$

ALTERNATIVE EQUATIONS NEAR LIMITING VALUES

For $\gamma=0°$ and $\gamma=180°$, equations (11) and (12) are undefined as a consequence of the implicit assumption in the development of equation (4) that **l** and **m**, the directions to the sun and to the earth, are independent (nonparallel) vectors. These limiting values of the phase are, however, never reached in passive satellite photography as demonstrated below in connection with figure 6. The range of values of γ near 0° and 180°, excluded by those considerations, is sufficiently large to eliminate any computational difficulties that might be anticipated in the evaluation of the corrections of equations (11) and (12) near those singularities.

On the other hand, the zeros of sin δ, cos δ in the denominator of equations (11) and (12) are possible singularities and require a modification of equations (11) and (12) for the corresponding limiting values of δ. For $\delta=90°$, $d\alpha$ in equations (11) and (12) has a zero in the denominator corresponding to the fact that right ascension is meaningless at the pole, hence also its increment. This leaves as the only real difficulty the case of $\delta=0$ for which the given formulas for $d\delta$ become meaningless. The reason for this breakdown is the arbitrary choice of omitting dm_3 in setting up equations (9), and this is the only component of the vector $d\mathbf{m}$ that affects $d\delta$ when $\delta=0$, as is apparent from equations (8). For $\delta=0$ therefore, as well as for values near 0, it will be necessary to determine $d\delta$ from the third of equations (8),

$$d\delta = \frac{dm_3}{\cos\delta} = \frac{\rho(\cos\gamma-1)}{2D\sin\gamma\cos\delta}(l_3 + m_3\cos\gamma)$$

or

$$d\delta = \frac{\rho(\cos\gamma-1)}{2D\sin\gamma\cos\delta}(\sin\delta_\odot + \cos\gamma\sin\delta). \tag{11'}$$

This equation is an optional alternative for the second of equations (11), computable for $\delta=0$ and preferable in that region of δ. Except at the limits, both yield identical results.

The corresponding equation for the case of specular reflection, equations (12), is

$$d\delta = -\frac{\rho}{D\sin\gamma\cos\delta}\left(\frac{1-\cos\gamma}{2}\right)^{1/2}(\sin\delta_{\odot}+\cos\gamma\sin\delta). \tag{12'}$$

Satellite triangulation depends on the astronomer's star catalog for basic data but, unlike metric astronomy, it operates and computes in three-dimensional space with a Euclidean metric, that is, with a Cartesian coordinate system. The singularities that require special consideration are, for the most part, singularities of the astronomer's two-dimensional curvilinear coordinate system which would be avoided by dropping the α, δ concept and spherical trigonometry at the earliest possible opportunity and by adopting the methods of analytic geometry, preferably vector analysis and matrix calculus. Experience at the National Ocean Survey has shown that a great many computational programs can be simplified by such a break with traditional concepts, in addition to giving a clearer picture of the basically simple geometric concepts involved. In the case presented here, for example, once an expression for the camera direction has been derived in the form of vector equations (2), there is really no need for explicit increments to α and δ. The increments dm_1, dm_2, dm_3 of equations (10), when added to **m** of equations (2), produce $\mathbf{m}+d\mathbf{m}$ which is equal to $\mathbf{m}(\alpha+d\alpha,\ \delta+d\delta)$; the trigonometric functions involved are simpler than those required for $d\alpha$ and $d\delta$ and are of general application for all values of α and δ.

Again, the zero in the denominator for $\gamma=0°$ and $180°$ makes the correction incomputable for these values of γ. Examination of figure 1 shows that the corresponding phases are "full moon" and "new moon," respectively. In the first case, the phase correction would be zero; and in the second, no photograph is possible.

The following geometric considerations establish limits for the neighborhoods of these points ($\gamma=0°$, $180°$) within which the passive satellite cannot be photographed. In figure 5, the location of the camera is at E and the sun is on the horizon at elevation 0, as indicated. For a given fixed elevation, the satellite may occupy any of the positions of the circle S, S_m, S_M.

As S assumes various positions, the angle γ at S, formed by the directions from S to E and from S to the sun, varies continuously, increasing from a minimum equal to the elevation of the satellite e_{sat} at the position S_m to a maximum at the position S_M where γ is the supplement of e_{sat}. The points S_m, S_M are in the vertical plane of the satellite containing the direction to the sun, that is, when the azimuths of the sun $\alpha_{\odot}$ and of the satellite α differ by 0° and 180°, respectively. If the angle of elevation or depression $e_{\odot}$ of the sun is different from zero, but still fixed, the same argument applies except that for every position of the satellite the corresponding angle is $\gamma+e_{\odot}$. We conclude, therefore, that to determine the extremal values of γ for given elevations of the sun and satellite, it is sufficient, as well as necessary, to consider the situation when sun and satellite are in the same vertical plane—the plane of figure 6.

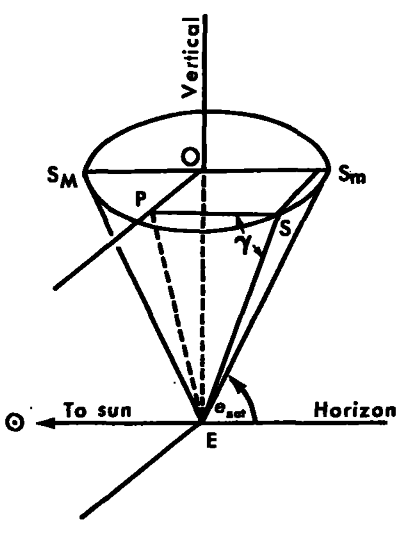

[The length of the generator SE is unity. In right ΔSPE: PS = cos $\angle$ PSE = cos γ. cos γ has maximum when S is at S_m.]

Figure 5.—Cone of constant satellite elevation.

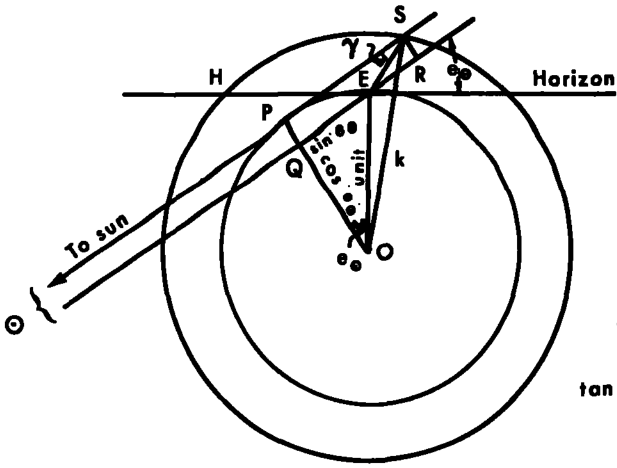

$$\gamma_{min} = \angle PSE = \angle RES$$

$$\tan \gamma_{min} = \frac{RS}{ER} = \frac{OP - OQ}{PS - QE} = \frac{1 - \cos e_\odot}{\sqrt{k^2 - 1} - \sin e_\odot}$$

Figure 6.—Minimal phase angle for passive satellite.

In figure 6, the camera is again at E on the surface of the terrestrial sphere with unit radius. The sun has an assumed minimal angle of depression $e_\odot$ to meet the physical conditions of the problem and the satellite moves in a circular orbit, concentric with the earth and radius $k>1$. The sun's rays graze the earth at P, and the extension of this direction through the point S on the satellite orbit delineates the umbra for near-earth satellites. For such a satellite with an elevation $e = e_\odot$, the angle γ would indeed be zero, but the satellite would be in the earth's shadow and hence excluded from consideration in passive satellite photography. The satellite emerges from the shadow at S. A perpendicular from S onto a line parallel to PS through E creates the right triangle ERS so that $\angle RES = \angle ESP$, which is the minimal angle γ for this critical point S of the orbit. The angle $QOE = e_\odot$, and therefore $QE = \sin e_\odot$, $OQ = \cos e_\odot$. From right triangle OPS, we have $PS = \sqrt{k^2 - 1}$.

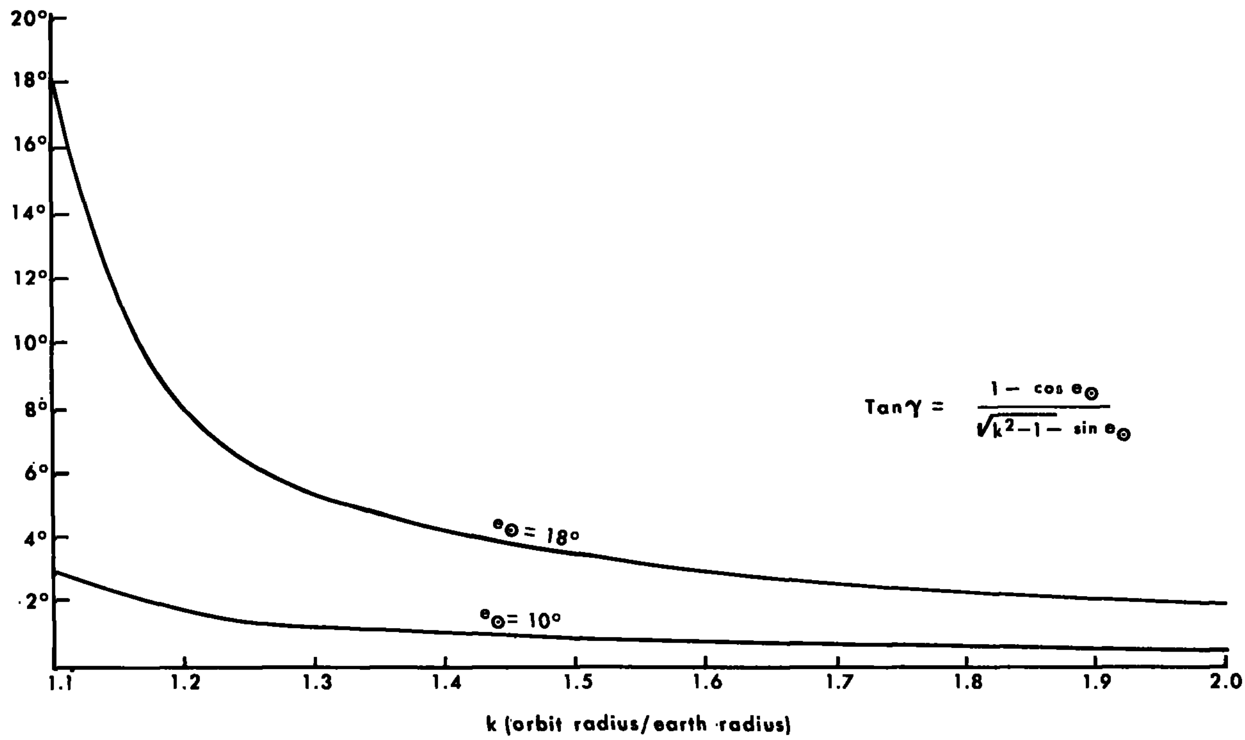

Figure 7.—Minimum phase angle.

Hence,

$$\tan\gamma = \tan\angle RES$$
$$= \frac{RS}{ER} = \frac{QP}{QR - QE} = \frac{OP - OQ}{PS - QE}$$

or

$$\tan\gamma = \frac{1 - \cos e_{\odot}}{\sqrt{k^2 - 1} - \sin e_{\odot}}. \qquad (13)$$

The minimum value of γ for a given angle of depression of the sun $e_{\odot}$ and for a given ratio k of the orbit radius to the earth's radius can be computed from this equation. The corresponding elevation of the satellite at point S_m (of fig. 5) will be $e_{sat} = e_{\odot} + \gamma$ (from fig. 6). The satellite remains visible and in sunlight until it reaches the horizon point H. At H, γ reaches a maximum of $180° - e_{\odot}$ which is therefore an upper bound for the phase angle corrections.

The graph of figure 7 shows minimum values of γ derived from equation (13), with the assumed minimum angles of depression $e_{\odot}$ of the sun equaling 10° and 18°, respectively, and the values of k varying from 1.1 to 2.

☆ U.S. GOVERNMENT PRINTING OFFICE: 1971 O—440-358

(Continued from inside front cover)

*C&GS 30. Cable Length Determinations for Deep-Sea Oceanographic Operations. Capt. Robert C. Darling, June 1966.

*C&GS 31. The Automated Standard Magnetic Observatory. L. R. Alldredge and I. Saldukas, June 1966.

ESSA TECHNICAL REPORTS—C&GS

*C&GS 32. Space Resection in Photogrammetry. M. Keller and G. C. Tewinkel, September 1966.

*C&GS 33. The Tsunami of March 28, 1964, as Recorded at Tide Stations. M. G. Spaeth and S. C. Berkman, July 1967.

*C&GS 34. Aerotriangulation: Transformation of Surveying and Mapping Coordinate Systems. Lt. Cdr. Melvin J. Umbach, July 1967.

*C&GS 35. Block Analytic Aerotriangulation. M. Keller and G. C. Tewinkel, November 1967.

*C&GS 36. Geodetic and Grid Angles—State Coordinate Systems. Lansing G. Simmons, January 1968.

*C&GS 37. Precise Echo Sounding in Deep Water. G. A. Maul, January 1969.

*C&GS 38. Grid Values of Total Magnetic Intensity IGRF—1965. E. B. Fabiano and N. W. Peddie, April 1969.

C&GS 39. An Advantageous, Alternative Parameterization of Rotations for Analytical Photogrammetry. Allen Pope, April 1970. Price $0.30.

C&GS 40. A Comparison of Methods of Computing Gravitational Potential Derivatives. L. J. Gulick, September 1970. Price $0.40.

NOAA TECHNICAL REPORTS—NOS

C&GS 41. A User's Guide to a Computer Program for Harmonic Analysis of Data at Tidal Frequencies. R. E. Dennis and E. E. Long, July 1971. Price $0.40.

C&GS 42. Computational Procedures for the Determination of a Simple Layer Model of the Geopotential From Doppler Observations. Bertold U. Witte, April 1971. Price $0.65.